Title: A derivation error that affects carbon balance models exists in the current implementation of the modified Arrhenius function

Running Title: Derivation error in modified Arrhenius model

Author: Bridget Murphy[1,2], Joseph R. Stinziano[3,*]

Affiliations: [1] Department of Biology, University of Western Ontario, London, ON, Canada; [2] Current Affiliation: Department of Cell and Systems Biology, University of Toronto, Toronto, ON, Canada; [3] Department of Biology, University of New Mexico, Albuquerque, NM, USA

[*] Corresponding author; Email: jstinziano@unm.edu; Tel: +1 (226) 678-1670

Article Type: Modelling/Theory

Word Count: 3,623

Introduction: 559

Description: 1640

Results: 688

Discussion: 710

Acknowledgments: 26

Number of Tables: 3

Number of Figures: 4

Supplementary Files: 1

Summary

- Understanding biological temperature responses is crucial to predicting global carbon fluxes. The current approach to modelling temperature responses of photosynthetic capacity in large scale modelling efforts uses a modified Arrhenius equation.
- We rederived the modified Arrhenius equation from the source publication from 1942 and uncovered a missing term that was dropped by 2002. We compare fitted temperature response parameters between the correct and incorrect derivation of the modified Arrhenius equation.
- We find that most parameters are minimally affected, though activation energy is impacted quite substantially. We then scaled the impact of these small errors to whole plant carbon balance and found that the impact of the rederivation of the modified Arrhenius equation on modelled daily carbon gain causes a meaningful deviation of ~18% day^{-1}.
- This suggests that the error in the derivation of the modified Arrhenius equation has impacted the accuracy of predictions of carbon fluxes at larger scales since >40% of Earth System Models contain the erroneous derivation. We recommend that the derivation error be corrected in modelling efforts moving forward.

Keywords: Arrhenius, temperature, photosynthesis, gas exchange, modelling, carbon balance

Introduction

Globally, photosynthesis and autotrophic respiration are the largest biological carbon fluxes, with photosynthesis removing ~120 Gt C year^{-1} from the atmosphere and autotrophic respiration releasing ~60 Gt C year^{-1} back to the atmosphere (Amthor, 2000; Ciais *et al.*, 2013). Given the temperature sensitivity of these large carbon fluxes (Lombardozzi *et al.*, 2015), understanding how photosynthesis and respiration respond on acute, acclimatory, and adaptive timescales is crucial for predicting vegetative and carbon cycle responses to future global climates (Rogers *et al.*, 2017; Stinziano *et al.,* 2018). Biological temperature responses including photosynthesis and respiration are typically assumed to be exponential or peaked (Way & Yamori, 2014; Smith & Dukes, 2017; Kumarathunge *et al.*, 2019). Exponential responses are usually modelled based on an Arrhenius-type curve (Arrhenius, 1915):

$$f(T) = k \exp\left(\frac{-E_a}{RT}\right) \qquad \text{Equation 1,}$$

or equivalently,

$$f(T) = k_{25} \exp\left[\frac{E_a(T-298.15)}{298.15RT}\right] \qquad \text{Equation 2}$$

where f(T) is the rate of the process at temperature T, k is a pre-exponential factor, E_a is the activation energy in J mol^{-1}, R is the universal gas constant of 8.314 J mol^{-1} K^{-1}, T in K, k_{25} is the rate of the process at 298.15 K, and 298.15 is the reference temperature in degrees Kelvin (K). As for peaked responses, while a few options are available (Kruse *et al.,* 2008; Hobbs *et al.*, 2013; Heskel *et al.*, 2016), the most commonly implemented version is the modified Arrhenius model of Johnson *et al.* (1942) as presented in Medlyn *et al.* (2002):

$$f(T) = k_{25} \exp\left[\frac{E_a(T-298.15)}{298.15RT}\right]\left[\frac{1+\exp\left(\frac{298.15\Delta S-H_d}{298.15R}\right)}{1+\exp\left(\frac{T\Delta S-H_d}{RT}\right)}\right] \qquad \text{Equation 3}$$

where H_d is the deactivation energy in J mol^{-1}, and ΔS is the entropy of the process in J mol^{-1} K^{-1}.

Equation 3 (**which will be referred to as M2002 from this point forward as it is conventionally referred to in the literature as the source of the equation**) is used for modelling the temperature responses of photosynthetic capacity (i.e. maximum carboxylation capacity of rubisco, V_{cmax}, maximum electron transport capacity, J_{max}, and triose phosphate utilization capacity (TPU); see Table 1 for a review of which Earth System Models use M2002). These parameters are then used in ecophysiological studies to understand thermal acclimation of photosynthesis (see Kattge & Knorr, 2007; Smith & Dukes, 2017; and Kumarathunge *et al.,* 2019 for examples). Furthermore, this equation is also used in terrestrial biosphere models to predict future carbon cycling (e.g. Rogers *et al.*, 2017).

Due to the ubiquity of M2002 in modelling temperature responses and the thermal acclimation of photosynthetic capacity (e.g. Kattge & Knorr, 2007; Rogers *et al.*, 2017; Smith & Dukes, 2017; Kumarathunge *et al.*, 2019; Table 1), we revisited the original Johnson *et al.* (1942) modified Arrhenius function to rederive M2002. In the process of this rederivation, we uncovered a term that was completely dropped sometime between Johnson *et al.* (1942) and Medlyn *et al.* (2002) which causes a systematic error in the application of the modified Arrhenius for modelling photosynthetic capacity in individual species (e.g. Medlyn *et al.*, 2002) to modelling global scale carbon uptake (e.g. Rogers *et al.*, 2017; Table 1). We then refit a freely available dataset (Kumarathunge *et al.*, 2019), with both versions of the modified Arrhenius model, and fed the temperature response fits through a carbon balance model to estimate the impact of the derivation error on modelled plant carbon balance. We predicted that the derivation error would cause substantial variation in fitted temperature response parameters, and that these differences would propagate through to modelled daily carbon balance.

<u>Description</u>

Rederivation of the modified Arrhenius equation

Johnson *et al.* (1942, equation 24) describe the temperature response of the light intensity of a luciferase reaction whereby the enzyme reversibly denatures or inactivates at high temperatures as:

$$I = \frac{c''T\exp\left(\frac{-\Delta H\ddagger}{RT}\right)}{1+\exp\left(\frac{\Delta S}{R}\right)\exp\left(\frac{-\Delta H}{RT}\right)} \qquad \text{Equation 4}$$

where I is the intensity of the luciferase reaction, c'' is not explicitly defined in Johnson *et al.* (1942), but appears to represent a constant based on the derivation of Equation 4, T is the temperature in K, R is the universal gas constant of 8.314 J mol^{-1} K^{-1}, ΔH‡ is the activation energy in J mol^{-1}, ΔH is the deactivation energy in J mol^{-1}, and ΔS is the entropy in J mol^{-1} K^{-1}. First, we harmonize the notation with standard ecophysiological representations such that ΔH‡ becomes E_a, and ΔH becomes H_d:

$$f(T) = \frac{c''T\exp\left(\frac{-E_a}{RT}\right)}{1+\exp\left(\frac{\Delta S}{R}\right)\exp\left(\frac{-H_d}{RT}\right)} \qquad \text{Equation 5}$$

We can relativize the equation to a reference temperature by dividing Equation 5 at a hypothetical temperature by Equation 5 at a standard temperature (i.e. 25 °C):

$$\frac{f(T)}{k_{25}} = \frac{\left[\frac{c''T\exp\left(\frac{-E_a}{RT}\right)}{1+\exp\left(\frac{\Delta S}{R}\right)\exp\left(\frac{-H_d}{RT}\right)}\right]}{\left[\frac{c''298.15\exp\left(\frac{-E_a}{298.15R}\right)}{1+\exp\left(\frac{\Delta S}{R}\right)\exp\left(\frac{-H_d}{298.15R}\right)}\right]} \qquad \text{Equation 6}$$

Next, rearrange fractions so that there is one numerator and one denominator on each line for clarity:

$$\frac{f(T)}{k_{25}} = \left[\frac{c''T\exp\left(\frac{-E_a}{RT}\right)}{c''298.15\exp\left(\frac{-E_a}{298.15R}\right)}\right]\left[\frac{1+\exp\left(\frac{\Delta S}{R}\right)\exp\left(\frac{-H_d}{298.15R}\right)}{1+\exp\left(\frac{\Delta S}{R}\right)\exp\left(\frac{-H_d}{RT}\right)}\right] \qquad \text{Equation 7}$$

Cancel out the constant c'', use exponent rules to simplify so that E_a is contained within a single exponential function, and the ΔS and H_d terms are grouped together:

$$\frac{f(T)}{k_{25}} = \frac{T}{298.15}\exp\left(\frac{-E_a}{RT} - \right)\left[\frac{1+\exp\left(\frac{\Delta S}{R}+\frac{-H_d}{298.15R}\right)}{1+\exp\left(\frac{\Delta S}{R}+\frac{-H_d}{RT}\right)}\right] \qquad \text{Equation 8}$$

Simplify further by setting a common denominator within exponential terms:

$$f(T) = k_{25}\frac{T}{298.15}\exp\left(\frac{-298.15E_a+E_aT}{298.15RT}\right)\left[\frac{1+\exp\left(\frac{298.15\Delta S-H_d}{298.15R}\right)}{1+\exp\left(\frac{T\Delta S-H_d}{RT}\right)}\right] \qquad \text{Equation 9}$$

Simplify exponential terms further to reduce the number of instances that E_a appears in the equation:

$$f(T) = k_{25}\frac{T}{298.15}\exp\left(\frac{E_a(T-298.15)}{298.15RT}\right)\left[\frac{1+\exp\left(\frac{298.15\Delta S-H_d}{298.15R}\right)}{1+\exp\left(\frac{T\Delta S-H_d}{RT}\right)}\right] \qquad \text{Equation 10}$$

Note the difference between M2002 and the rederived equation 10 (**which will be referred to as J1942**): the term T / 298.15 is missing from M2002. There are several alternative expressions of Equation 4 (e.g. Farquhar *et al*., 1980; Harley *et al.*, 1986; Harley *et al.*, 1992; Harley & Baldocchi, 1995; Lloyd, 1995), however when relativized to a common temperature, the equations presented in Farquhar *et al.* (1980), Harley *et al.* (1992), Harley & Baldocchi (1995), and Lloyd (1995) are all identical to M2002 when relativized by temperature, while the Harley *et al.* (1986) equation is identical to our derivation (J1942) when relativized to a common temperature (see Appendix A for the relativizations of Farquhar *et al.* (1980), Harley *et al.* (1986), and Harley *et al.* (1992); Harley & Baldocchi (1995) uses an identical equation to Eq. 18 from Medlyn *et al.* (2002), while Lloyd (1995) uses an identical equation to Eq. 17 from Medlyn *et al.* (2002)).

We traced the origin of the dropped term to two papers: Hall (1979) and Farquhar et al. (1980). Both papers cite the M2002 equation as belonging to Sharpe and DeMichele (1977) when in fact it belongs to Johnson et al. (1942). In Hall (1979), the reasoning behind the dropped term is given as: “In addition their linear T term was omitted because it has little influence on the function and would have prevented Eq. 22 [the M2002 equation] from approaching Eq. 21 [Equation 1 in the present study] in

the limiting conditions of low temperatures" (Hall, 1979, page 305). Considering J1942, at 5 °C the error due to the dropped term would be ~278 K / 298 K = ~0.93, and at 45 °C would be 318 K / 298 K = ~1.07, so ~7% error at those temperatures. In context of measurement precision, such an assumption of "little influence" may have been reasonable at the time. However, the reason regarding the convergence of the two equations is simply tuning the model equations to fit their expectations. Meanwhile, Farquhar et al. (1980) report that: "Eq. (36) is a simplified version of an equation developed by Sharpe and DeMichelle [sic] (1977) to describe the effect of temperature on enzyme inactivation" (Farquhar et al., 1980, page 84). In both cases, it appears that the intention was to simplify the equation, which in the process of simplifying, generated an error that was propagated for over 40 years.

The derivation error introduces multiple systematic errors. First, errors are introduced into the fitted parameters E_a, H_d, and ΔS. Second, k_{25} is scaled using the wrong equation, introducing an error in f(T). And third, acclimation equations describing E_a, H_d, and ΔS will then be in error due to errors in the fitted parameters at each temperature. Here we focus on the impact of the dropped term on fitted temperature response parameters and modelling whole-plant carbon balance.

Data analysis

Using A-C_i curve data compiled in Kumarathunge *et al.* (2019), available from the Kumarathunge *et al.* (2018) repository, we used the {fitacis} function from the R package {plantecophys} (Duursma, 2015), setting fitmethod = "bilinear", Tcorrect = FALSE, and fitTPU = TRUE, to obtain V_{cmax} and J_{max}. We then fit Equations 3 and 10 to the data, allowing H_d to be fit. To ensure that the curves could be fit (i.e. that there were enough data to fit 4 parameters), we only used data where A-C_i curves were measured at 5 or more temperatures. This reduced the number of candidate temperature responses from 729 to 403. We used the R package {minpack.lm} (Elzhov *et al.,* 2016), using Equation 2 to obtain starting values for E_a and k_{25}, while the other initial parameters were ΔS = 0.650 kJ mol^{-1} K^{-1}, and H_d varying from 1 to 1000 kJ mol^{-1}, followed by the {BIC} function to select the best model based on Bayesian Information Criteria. We obtained 341 and 337 successful V_{cmax} temperature response curve fits for M2002 and J1942, respectively, and 241 and 242 successful J_{max} temperature response curve fits for M2002 and J1942, respectively. This resulted in a total of 547 fitted temperature response curves

which we filtered further, requiring that E_a, ΔS, and H_d were all positive values and that the V_{cmax} and J_{max} data were paired, resulting in 196 complete pairs of V_{cmax} and J_{max} temperature responses for analysis. The data covered a temperature range from 1 °C to 50 °C across all curves, with a median range of 14 °C to 42.6 °C.

Modelling

We modelled the impact of the M2002 and J1942 equations on daily net plant carbon balance. Data for leaf area, root and shoot masses, as well as leaf dark respiration at 25 °C were taken for white spruce (*Picea glauca*) from Stinziano & Way (2017), while stomatal conductance model parameters were calculated with the gas exchange data reported in Stinziano & Way (2017). Briefly, Stinziano and Way (2017) grew white spruce in growth chambers under a simulated autumn treatment based on temperatures and photoperiods from Trenton, ON, with weekly harvesting of biomass and gas exchange measurements across 17 weeks as a control treatment, along with a warming treatment where temperatures were +5 °C of the control, a constant summer day/night temperature with declining photoperiod, and a constant summer photoperiod with ambient changes in temperature. Here we only used data from Stinziano & Way (2017) that were from the control treatment. Mean data were taken from the control treatment at weeks 0 and 12 to provide contrasting biomass allocation patterns such that week 0 is a low respiration scenario and week 12 is a high respiration scenario. These different respiration scenarios were used to reduce bias in any conclusions regarding the impact of the M2002 and J1942 equations on carbon balance, as the ratio of photosynthesis to respiration may alter the sensitivity of net carbon balance to the Arrhenius equation used. Root respiration for white spruce was taken from Weger & Guy (1991) and we assumed that stem respiration was equal to root respiration (Table 2).

For the full model structure and equations, please see the accompanying R package {arrhenius.comparison} ("arrhenius.comparison_1.0.2.tar.gz"; Stinziano & Murphy, 2020) (see Table 3 for equations). Briefly, we linked the Medlyn *et al.* (2011) stomatal conductance model with the Farquhar *et al.* (1980) C_3 photosynthesis model, assuming infinite mesophyll conductance to CO_2 as these same assumptions were used in fitting the data from Kumarathunge *et al.* (2018). Photosynthetic capacity, both maximum rubisco carboxylation capacity, V_{cmax}, and maximum electron

transport rate, J_{max}, were scaled to temperature using either M2002 or J1942, while respiration was scaled according to (Atkin & Tjoelker, 2003). Photosynthesis and respiration were summed across each modelled day to calculate daily plant carbon assimilation.

Modelling was performed on 18 total days of environmental data, with three days of data from three months (17th – 19th of May, August, and October, 2019) obtained from external irradiance sensors at the Biotron Experimental Climate Change Research Centre at the University of Western Ontario and the remaining environmental data from Environment Canada historical climate data for South London (43.01°N, 81.27°W, altitude: 251 m; temperature range: -0.1 – 27.9 °C) and the rooftop greenhouse at the University of New Mexico (35.08°N, 106.62°W, altitude: 1587 m; temperature range: 7.2 – 42.2 °C) to capture different levels of environmental variability (see *Impacts on modelled net carbon balance* for environmental data).

Overall, the modelling approach allows us to assess the relative differences between Equations 3 and 10 under a low- and high- respiration scenario across different ranges of seasonal variability.

Statistical analysis

Data were analyzed using the {lm} function in R v.3.6.2 (R Core Team, 2019), regressing the data obtained from M2002 against the data obtained from J1942 for each of $V_{cmax,25}$, $J_{max,25}$, $E_{a,Vcmax}$, $E_{a,Jmax}$, ΔS_{Vcmax}, ΔS_{Jmax}, $H_{d,Vcmax}$, $H_{d,Jmax}$, BIC values for the fits of Equations 3 and 10, daily photosynthesis, daily net carbon balance, and daily photosynthesis : daily respiration ratios. Intercepts in the regression, when significant, were interpreted as a bias in the parameter, while deviations in slope from a 1:1 relationship where interpreted as percentage over- or under- estimation of the parameter (i.e. [parameter slope – 1] · 100 = % estimation error). All p-values were corrected for multiple testing using the p.adjust() function in R with Holm's method. All code and data will be made freely available on GitHub upon publication in the {arrhenius.comparison} R package (Stinziano & Murphy, 2020).

Results

Equations M2002 and J1942 exhibited similar performance

233 The performance between M2002 and J1942 for fitting $V_{cmax,25}$ temperature responses were
234 essentially identical when assessed based on BIC, with a slope of 1.001 ± 0.001 ($F_{1,195}$ = 5.52 · 10^5, R^2 =
235 0.9996, P < 2.2 · 10^{-16}; Fig. **1a**), as was the case for $J_{max,25}$ with a slope of 1.001 ± 0.001 ($F_{1,195}$ = 2.43 ·
236 10^6, R^2 = 0.9999, P < 2.2 · 10^{-16}; Fig. **1b**). However, while fitted temperature responses based on BIC
237 appeared identical, the largest discrepancy between fitted responses was observed when comparing
238 $J_{max,25}$ of both plant species scaled across 10 ˚C and 50 ˚C (Figs. **1c-f**; note the differences between the
239 blue and red hatched lines).
240
241 Estimates of $V_{cmax,25}$ were essentially identical between the M2002 fitting (y-axis) and the J1942 fitting
242 (x-axis) with a slope of 1.002 ± 0.004 ($F_{1,195}$ = 5.84 · 10^4, R^2 = 0.9967, P < 2.2 · 10^{-16}; Fig. **2e**), as was the
243 case for $J_{max,25}$ with a slope of 1.001 ± 0.001 ($F_{1,195}$ = 6.56 · 10^5, R^2 = 0.9997, P < 2.2 · 10^{-16}; Fig. **2f**).
244 $E_{a,Vcmax}$ was generally underestimated with a slope of 0.847 ± 0.024 and a positive bias of 9.73 ± 2.59
245 kJ mol^{-1} when using M2002 ($F_{1,194}$ = 1202, R^2 = 0.8610, P < 2.2 · 10^{-16}; Fig. **2a**), while $E_{a,Jmax}$ was
246 underestimated with a slope of 0.832 ± 0.013 and a positive bias of 5.98 ± 1.06 kJ mol^{-1} ($F_{1,194}$ = 3834,
247 R^2 = 0.9518, P < 2.2 · 10^{-16}; Fig. **2b**). ΔS_{Vcmax} was essentially identical between M2002 and J1942 with a
248 slope of 1.000 ± 0.0233 ($F_{1,195}$ = 1849, R^2 = 0.9046, P < 2.2 · 10^{-16}; Fig. **2c**), as was the case with ΔS_{Jmax}
249 with a slope of 0.988 ± 0.033 ($F_{1,195}$ = 904, R^2 = 0.8226, P < 2.2 · 10^{-16}; Fig. **2d**), and $H_{d,Vcmax}$ with a slope
250 of 1.002 ± 0.005 ($F_{1,195}$ = 4.12 · 10^4, R^2 = 0.9953, P < 2.2 · 10^{-16}; Fig. **2g**). However, $H_{d,Jmax}$ was
251 underestimated with a slope of 0.952 ± 0.024 and a positive bias of 31.48 ± 8.93 kJ mol^{-1} ($F_{1,194}$ = 1592,
252 R^2 = 0.8914, P < 2.2 · 10^{-16}; Fig. **2h**).
253
254 *Impacts on modelled net carbon balance*
255 In general, the differences in thermal response parameters were amplified when integrated at the
256 whole-plant level across a range of environmental conditions (Fig. **3**). For modelled daily
257 photosynthesis (A), the slope for the low respiration model was 0.819 ± 0.013 and the intercept was
258 0.018 ± 0.002 g $plant^{-1}$ day^{-1} (M2002 versus J1942; approximately 18% of modelled A) ($F_{1,3523}$ = 4.168 ·
259 10^3, R^2 = 0.5418; P < 2.2 · 10^{-16}) (Fig. **4a**). For the high respiration model of daily A, the slope was 0.819
260 ± 0.013 and the intercept was 0.031 ± 0.003 g $plant^{-1}$ day^{-1} (approximately 18% of modelled A) ($F_{1,3523}$
261 = 4.168 · 10^3, R^2 = 0.5418; P < 2.2 · 10^{-16}) (Fig. **4b**). The low respiration model of total daily carbon (C)
262 gain had a slope of 0.836 ± 0.012 and an intercept of 0.012 ± 0.001 g $plant^{-1}$ day^{-1} (approximately 16%

263 of modelled C gain) (M2002 versus J1942; $F_{1,3523} = 4.539 \cdot 10^3$, $R^2 = 0.5629$; $P < 2.2 \cdot 10^{-16}$) (Fig. **4c**). The
264 high respiration of total C gain similarly had a slope of 0.859 ± 0.012 and an intercept of 0.011 ± 0.002
265 g plant^{-1} day^{-1} (approximately 14% of modelled C gain) (M2002 versus J1942; $F_{1,3523} = 5.364 \cdot 10^3$, R^2 =
266 0.6035; $P < 2.2 \cdot 10^{-16}$) (Fig. **4d**). The ratio of the total daily photosynthesis: respiration (A/R) was also
267 considered when comparing models. The low respiration model of A/R had a slope of 0.982 ± 0.007
268 and the intercept was 0.146 ± 0.031 (approximately 2% of modelled A/R) (M2002 versus J1942; $F_{1,3523}$
269 $= 2.096 \cdot 10^4$, $R^2 = 0.8561$; $P < 2.2 \cdot 10^{-16}$) (Fig. **4e**). The high respiration model had a similar slope of
270 0.982 ± 0.007 and the intercept was 0.082 ± 0.017 (approximately 2% of modelled A/R) (M2002
271 versus J1942; $F_{1,3523} = 2.097 \cdot 10^4$, $R^2 = 0.8562$; $P < 2.2 \cdot 10^{-16}$) (Fig. **4f**).
272

273 **Discussion**

274 We sought to determine whether the missing term in M2002 had a meaningful impact on fitted
275 temperature response parameters due to its prevalence in photosynthetic temperature response data
276 and vegetation modelling (Kattge & Knorr, 2007; Duursma & Medlyn, 2012; Rogers *et al.,* 2017; Smith
277 & Dukes, 2017; Stinziano *et al.,* 2018; Stinziano *et al.,* 2019; Kumarathunge *et al.,* 2019). Our present
278 analysis suggests that there is a large impact on E_a for both V_{cmax} and J_{max}, however there were
279 minimal impacts on k_{25}, H_d, and ΔS (though note that $H_{d,Jmax}$ was underestimated) (Fig. **2**). In general,
280 fitting M2002 instead of J1942 results in E_a reductions of around 15% with positive bias, even though
281 fitted responses are *visually* similar (Fig. **1**). These findings are promising in that one of the
282 parameters to which modelled carbon gain is particularly sensitive, H_d (Stinziano *et al.,* 2018), is
283 minimally affected by the missing term. However, since temperature responses are non-linear, small
284 changes in the shape of an accelerating curve can have a strong impact on the integral of the
285 response (Jensen, 1906; e.g. changes in the shape of the temperature response of carbon assimilation
286 can have strong impacts on total carbon fixation). Despite fit performance being nearly identical and
287 visually similar (Fig. **1**), the differences due to E_a values between the equations led to an 18%
288 reduction in modelled daily photosynthesis for M2002 compared to J1942, leading to a ~14-16%
289 reduction in modelled net daily carbon gain. Overall, comparisons of low-respiration to high-
290 respiration scenarios resulted in similar percent changes in daily C balance with similar variation.
291

Not only did we compare the impact of the missing term in M2002 on different respiration scenarios, but we also modelled data across a range of environmental conditions to understand the impact on C balances of plants under different temperature regimes and how these impacts could scale up in global models. A ~15% reduction in net daily carbon gain is substantial by itself, but this difference would also be amplified over time for a single plant. Plant growth follows the compound interest law (Blackman, 1919). As leaf area increases with growth so too does the rate of photosynthesis and thus the amount of carbon available to further increase growth and metabolism, hence why relative growth rates are commonly utilized in the literature (e.g. Shipley, 1989; Causton, 1991; Tjoelker *et al.*, 1999; Loveys *et al.,* 2003; Poorter *et al.,* 2012; Pommereng & Anders, 2015). A reduction of 18% in modelled daily photosynthesis caused by using the modified equation with the missing term (M2002) would become compounded long-term with plant growth and may result in underestimations of future carbon uptake. It is thus likely that the differences we observed would accumulate to even larger carbon flux errors across large spatial and temporal scales with fluctuating temperatures.

Based on the above analysis, the impact of the missing term in the modified Arrhenius equation substantially alters E_a and net daily carbon balance at a whole-plant level. While our models of plant carbon uptake were indicative of problems caused by using M2002, it would be worth comparing how the use of this derivation has affected the interpretation of temperature response data and whole plant carbon balances collected from previous studies. Future work comparing the impact of using M2002 opposed to J1942 on interpreting whole tree carbon balance and net primary production data could lead to better estimations of the temperature sensitivity of carbon uptake. Given that carbon balance is the time integral of net CO_2 assimilation, this may also lead to substantial impacts over a long time period. On a larger scale, a correction of this derivation error will also be necessary when considering Earth system models, as 17 out of 40 models in the CMIP6 simulations are affected by the derivation error (Table 1). We therefore recommend the switch from M2002 to J1942 because: 1) M2002 is the result of a derivation error circa 1979, and 2) M2002 and J1942 lead to different net daily carbon estimates due to the derivation error, which may currently be compensated by other factors in large-scale models, most notably in the Community Land Model which currently relies on the M2002 equation (Bonan, 1996; Lawrence et al., 2018) and underlies 30% of Earth System Models (Table 1).

Acknowledgments

We would like to thank Wesley J. Noe at the University of New Mexico for providing climate data. This research was supported by personal funds.

Author Contributions

Both authors contributed to all aspects of the study.

Additional Information

A version of this manuscript was posted on bioRxiv (manuscript ID: BIORXIV/2020/921973).

Tables

Table 1. List of land surface models affected by the derivation error in M2002 and the affected Earth Systems Models (ESMs) being used in the CMIP6 simulations. Note that 17 of the 40 (42.5%) CMIP6 ESMs are affected by the derivation error. Affected models are in bold.

Land Surface Model Family		# of ESMs	Contains M2002?	Affected ESMs	References
Atmosphere-Vegetation Interaction Model	AVIM	2	No	BCC-CSM2-MR, BCC-ESM1	Ji, 1995
Community Atmosphere-Biosphere Land Exchange Model	**CABLE**	**2**	**Yes**	**ACCESS-CM2, ACCESS-ESM1-5**	**Haverd et al., 2018**
Canadian Land Surface Scheme	**CLASS**	**1**	**Yes**	**CanESM5**	**Swart et al., 2019**
Community Land Model	**CLM**	**12**	**Yes**	**CAMS-CSM1-0, CESM2, CESM2-FV2, CESM2-WACCM, CESM2-WACCM-FV2, NorESM2-LM, NorESM2-MM, E3SM-1-0, FGOALS-f3-L, FGOALS-g3, TaiESM1, SAM0-UNICON**	**Bonan, 1996; Lawrence et al., 2018**
Goddard Institute for Space Studies Global Circulation Model	GISS-GCM	3	No	GISS-E2-1-G, GISS-E2-1-H, GISS-E2-2-G	Friend & Kiang, 2005
Interaction Soil Biosphere Atmosphere Carbon Cycle	ISBAcc	3	No	CNRM-CM6-1, CNRM-CM6-1-HR, CNRM-ESM2-1	Calvet et al., 1998; Joetzjer et al., 2015
Joint Scheme for Biosphere Atmosphere Coupling in Hamburg	JSBACH	4	No	AWI-CM-1-1-MR, MPI-ESM1-2-HR, MPI-ESM1-2-LR, NESM3	Rogers et al., 2017; Cao et al., 2018
Joint UK Land Environment Simulator	JULES	3	No	HadGEM3-GC31-LL, HadGEM-GC31-MM, UKESM	Clark et al., 2011
Land Model 4	LM4	2	No	GFDL-CM4, GFDL-ESM4	Milly et al., 2014
Lund-Potsdam-Jena Model	LPJ	3	No	EC-Earth3, EC-Earth3-Veg, IPSL-CM6A-LR	Sitch et al., 2003; Arora et al., 2020
Simple Biosphere Model	SiB	3	No*	INM-CM4-8, INM-CM5-0, MRI-ESM2-0	Sato et al., 1989; Volodin & Lykosov, 1998; Hosaka, 2011
Vegetation Integrative SImulator for Trace Gases	**VISIT**	**2**	**Yes**	**MIROC6, MIROC-ESL2**	**Ito, 2010; Arora et al., 2020**

*The SiB model does not include photosynthesis.

336 **Table 2. Parameters used in modelling daily carbon gain.**

Parameter	Group	Value	Reference
Respiration	R_{dark}	2.78 µmol m^{-2} s^{-1}	Stinziano & Way, 2017
	R_{day}	0.7 * R_{dark}	Ayub *et al.*, 2011
	R_{root}	0.0095 µmol g^{-1} s^{-1}	Weger & Guy, 1991
	R_{stem}	0.0095 µmol g^{-1} s^{-1}	Assumed
	Q_{10}	2.015	Atkin & Tjoelker, 2003
Γ*	25 °C	42.75 µmol mol^{-1}	Bernacchi *et al.*, 2001
	E_a	37.83 kJ mol^{-1}	Bernacchi *et al*., 2001
K_m	25 °C	718.4 µmol mol^{-1}	Bernacchi *et al.,* 2001
	E_a	65.51 kJ mol^{-1}	Bernacchi *et al.,* 2001
α		0.8	Norman & Campbell, 1998
ϕ		0.08	Norman & Campbell, 1998
Leaf Area	Low R	0.015 m^2	Stinziano & Way, 2017
	High R	0.025 m^2	Stinziano & Way, 2017
Stem Mass	Low R	0.496 g	Stinziano & Way, 2017
	High R	2.523 g	Stinziano & Way, 2017
Root Mass	Low R	0.498 g	Stinziano & Way, 2017
	High R	5.072 g	Stinziano & Way, 2017

337 **Q_{10}: thermal sensitivity coefficient; Γ*: photorespiratory CO_2 compensation point; K_m: apparent**
338 **Michaelis-Menten constant for rubisco carboxylation in 21% O_2/air (i.e. $K_{c,air}$); α: absorbance of**
339 **photosynthetically activation radiation; ϕ: maximum quantum efficiency of photosynthetic electron**
340 **transport; E_a: activation energy; R_{dark}: leaf respiration in the dark; R_{day}: leaf respiration in the light;**
341 **R_{root}: root respiration; R_{stem}: stem respiration; Low R: low respiration scenario; High R: high**
342 **respiration scenario.**
343
344

Table 3. Equations used in modelling daily carbon uptake.

Equation	Reference
$$f(T) = k_{25} Q_{10}^{\frac{T-298.15}{10}}$$	Atkin & Tjoelker, 2003
$$f(T) = k_{25} e^{\left[\frac{E_a(T-298.15)}{298.15RT}\right]}$$	Arrhenius, 1915
$$f(T) = k_{25} e^{\left[\frac{E_a(T-298.15)}{298.15RT}\right]} \left[\frac{1+e^{\frac{298.15\Delta S-H_d}{298.15R}}}{1+e^{\frac{T\Delta S-H_d}{RT}}}\right]$$	Medlyn *et al.*, 2002
$$f(T) = k_{25} \frac{T}{298.15} e^{\left[\frac{E_a(T-298.15)}{298.15RT}\right]} \left[\frac{1+e^{\frac{298.15\Delta S-H_d}{298.15R}}}{1+e^{\frac{T\Delta S-H_d}{RT}}}\right]$$	Johnson *et al.*, 1942; this study
$$W_c = V_{cmax} \frac{C_i - \Gamma *}{C_i + K_m}$$	Farquhar *et al.*, 1980
$$W_j = J\left(\frac{C_i - \Gamma *}{C_i + 2\Gamma *}\right)$$	Farquhar *et al.*, 1980; Way et al., 2011
Where J is calculated as the minimum root of: $\theta J^2 - (0.5\alpha\phi Q_{in} + J_{max})J + 0.5\alpha\phi Q_{in} J_{max} = 0$	
$$A_{gross} = min(W_c, W_j)$$	
$$A_{net} = A_{gross} - R_{day}$$	
$$g_s = g_0 + 1.6\left(1 + \frac{g_1}{\sqrt{VPD}}\right)\left(\frac{A_{net}}{C_a}\right)$$	Medlyn *et al.*, 2011
$$C_i = C_a - 1.6\frac{A_{net}}{g_s}$$	
$$A_{plant} = A_{net} \times LA - R_{dark} \times LA - R_{stem} \times SM - R_{root} \times RM$$	
$$C_{balance} = \sum A_{plant} \times 3600 \times \frac{12.01}{1{,}000{,}000}$$	

f(T): rate of a process at a given temperature; T: temperature in K; k_{25}: rate of a process at 25 °C; Q_{10}: thermal sensitivity coefficient; E_a: activation energy in kJ mol^{-1}; ΔS: entropy parameter in kJ mol^{-1}; H_d: deactivation energy in kJ mol^{-1}; R: universal gas constant in 0.008314 kJ mol^{-1} K^{-1}; W_c: rate of CO_2-limited carboxylation in µmol m^{-2} s^{-1}; W_j: rate of RuBP regeneration-limited carboxylation in

350 **μmol m^{-2} s^{-1}; V_{cmax}: maximum rate of rubisco carboxylation capacity in μmol m^{-2} s^{-1}; J_{max}: maximum**
351 **rate of electron transport in μmol m^{-2} s^{-1}; C_i: intercellular CO_2 concentration in μmol mol^{-1}; Γ*:**
352 **photorespiratory CO_2 compensation point in μmol mol^{-1}; K_m: Michaelis-Menten constant for rubisco**
353 **in μmol mol^{-1}; α: absorbance of photosynthetically active radiation; ϕ: maximum quantum**
354 **efficiency of electron transport; Q_{in}: incident photosynthetically active radiation; A_{gross}: gross CO_2**
355 **assimilation in μmol m^{-2} s^{-1}; A_{net}: net CO_2 assimilation in μmol m^{-2} s^{-1}; R_{day}: leaf day respiration in**
356 **μmol m^{-2} s^{-1}; g_s: stomatal conductance to water in mol m^{-2} s^{-1}; g_o: intercept for the Medlyn et al.**
357 **2011 model; g_1: slope for the Medlyn et al. 2011 model; VPD: vapor pressure deficit in kPa; C_a: CO_2**
358 **concentration at the leaf surface in μmol mol^{-1}; A_{plant}: whole plant net CO_2 assimilation; LA: leaf**
359 **area in m^{-2}; R_{dark}: leaf dark respiration in μmol m^{-2} s^{-1}; R_{stem}: stem respiration in μmol m^{-2} s^{-1}; R_{root};**
360 **root respiration in μmol m^{-2} s^{-1}; SM: stem mass in g; RM: root mass in g; $C_{balance}$: whole plant daily**
361 **carbon balance in g $plant^{-1}$ day^{-1}.**
362
363
364 **<u>Figure Captions</u>**
365 **Figure 1. Relative performance and fit for Equations 3 (M2002) and 10 (J1942) for temperature**
366 **responses of $V_{cmax\ 25}$ and $J_{max\ 25}$ based on a,b) Bayesian Information Criterion (BIC), and c-f) visual**
367 **inspection of curve fits across 10-50 ˚C for c,d) *Elymus canadensis* and 20-50 ˚C of e,f) *Betula***
368 ***alleghaniensis*. Red dashed lines indicate curves fitted with the M2002 equation and blue dotted**
369 **lines indicate curves fitted with the J1942 equation. Parameters for c-f) are as follows: c) M2002:**
370 **k_{25}: 46.4 μmol m^{-2} s^{-1}, E_a: 29.0 kJ mol^{-1}, ΔS: 0.692 kJ mol^{-1} K^{-1}, H_d: 221.4 kJ mol^{-1}; J1942: k_{25}: 46.4 μmol**
371 **m^{-2} s^{-1}, E_a: 29.0 kJ mol^{-1}, ΔS: 0.655 kJ mol^{-1} K^{-1}, H_d: 209.0 kJ mol^{-1}; d) M2002: k_{25}: 68.9 μmol m^{-2} s^{-1}, E_a:**
372 **0.0 kJ mol^{-1}, ΔS: 0.746 kJ mol^{-1} K^{-1}, H_d: 240.5 kJ mol^{-1}; J1942: k_{25}: 69.5 μmol m^{-2} s^{-1}, E_a: 0.0 kJ mol^{-1},**
373 **ΔS: 0.625 kJ mol^{-1} K^{-1}, H_d: 201.0 kJ mol^{-1}; e) M2002: k_{25}: 37.6 μmol m^{-2} s^{-1}, E_a: 57.7 kJ mol^{-1}, ΔS: 0.579**
374 **kJ mol^{-1} K^{-1}, H_d: 185.4 kJ mol^{-1}; J1942: k_{25}: 37.0 μmol m^{-2} s^{-1}, E_a: 57.7 kJ mol^{-1}, ΔS: 0.557 kJ mol^{-1} K^{-1},**
375 **H_d: 178.1 kJ mol^{-1}; f) M2002: k_{25}: 66.7 μmol m^{-2} s^{-1}, E_a: 23.0 kJ mol^{-1}, ΔS: 0.761 kJ mol^{-1} K^{-1}, H_d: 246.6**
376 **kJ mol^{-1}; J1942: k_{25}: 65.5 μmol m^{-2} s^{-1}, E_a: 23.0 kJ mol^{-1}, ΔS: 0.668 kJ mol^{-1} K^{-1}, H_d: 216.1 kJ mol^{-1}.**
377
378 **Figure 2. The modified Arrhenius equation missing the term (M2002) compared to J1942 fits**
379 **different values for E_a (a,b), but mostly similar values for ΔS (c,d), k_{25} (e,f) and H_d (f, g) for both V_{cmax}**

380 **(a, c, e, g) and J_{max} (c, d, f, h). E_a: activation energy, ΔS: entropy parameter, k_{25}: rate of the process**
381 **at 25 °C, H_d: deactivation energy, V_{cmax}: maximum capacity of rubisco carboxylation, J_{max}: maximum**
382 **rate of electron transport. Black line indicates 1:1 line and grey dashed line indicates respective**
383 **modelled slopes and intercepts.**
384
385 **Figure 3. Hourly environmental data used to drive the model in Table 3 covering 3 days (17th, 18th,**
386 **and 19th) of 3 months. (a,c,e) Albuquerque, NM, USA (ABQ); (b,d,e) London, ON, Canada (LDN).**
387 **Environmental parameters include: a,b) temperature; c,d) vapour pressure deficit; and e,f)**
388 **irradiance (Q_{in}).**
389
390 **Figure 4. The modified Arrhenius equation without the missing term (M2002) gives differences in**
391 **modelled daily carbon fluxes compared to J1942 for low R (a,c,e) and high R (b,d,f) under scenarios**
392 **where H_d is allowed to vary. Modelled carbon fluxes include: a,b) Total daily photosynthesis; c,d)**
393 **total daily C gain; and e,f) total daily A/R. A: photosynthesis, R respiration, Low R: low respiration,**
394 **High R: high respiration. Black line indicates 1:1 line and grey dashed line indicates respective**
395 **modelled slopes and intercepts.**
396
397

398 **Figures**

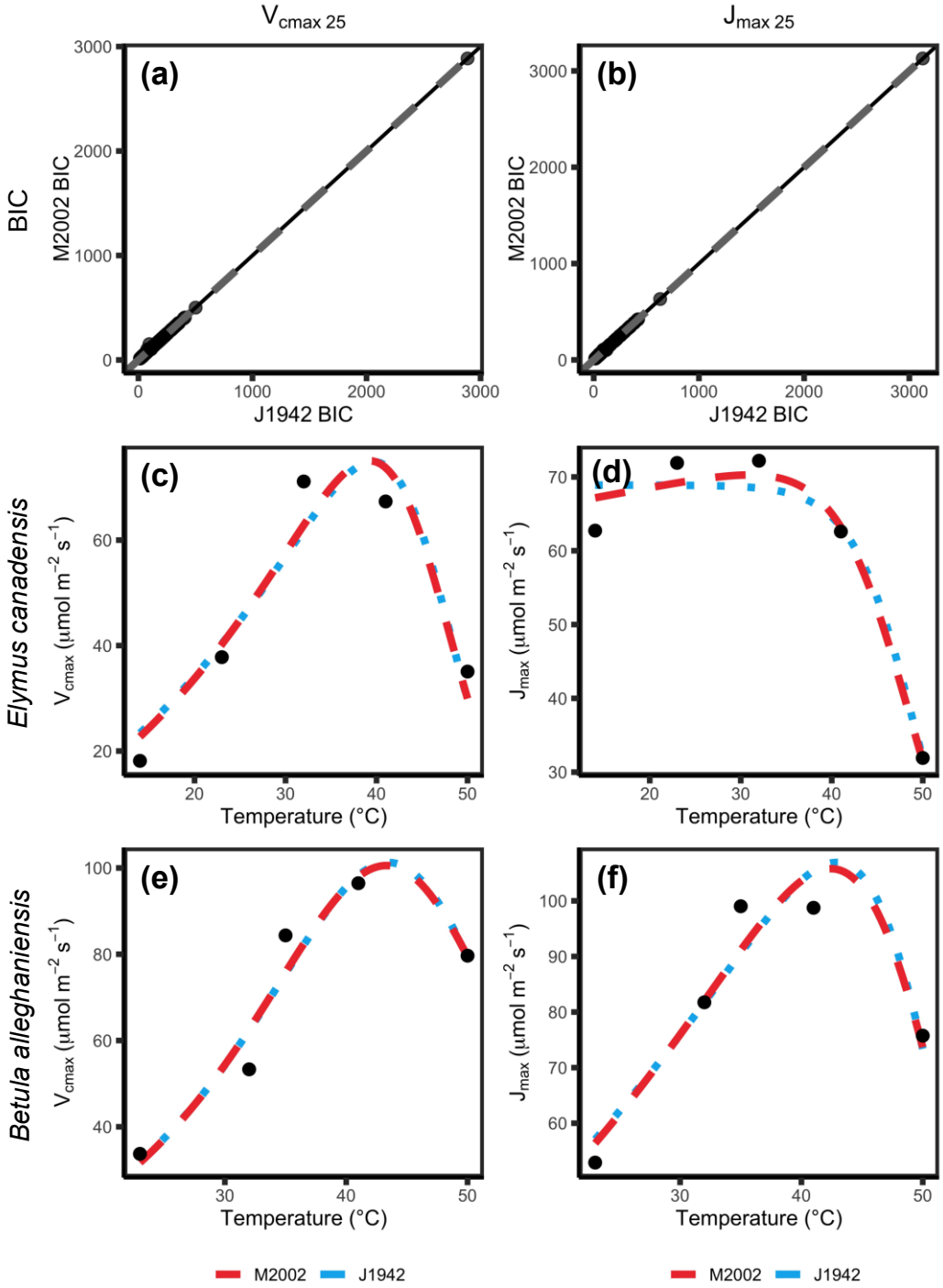

399

400 **Figure 1. Relative performance and fit for Equations 3 (M2002) and 10 (J1942) for temperature**
401 **responses of $V_{cmax\ 25}$ and $J_{max\ 25}$ based on a,b) Bayesian Information Criterion (BIC), and c-f) visual**
402 **inspection of curve fits across 10-50 ˚C for c,d) *Elymus canadensis* and 20-50 ˚C of e,f) *Betula***
403 ***alleghaniensis*. Red dashed lines indicate curves fitted with the M2002 equation and blue dotted**
404 **lines indicate curves fitted with the J1942 equation. Parameters for c-f) are as follows: c) M2002:**

k_{25}: 46.4 µmol m^{-2} s^{-1}, E_a: 29.0 kJ mol^{-1}, ΔS: 0.692 kJ mol^{-1} K^{-1}, H_d: 221.4 kJ mol^{-1}; J1942: k_{25}: 46.4 µmol m^{-2} s^{-1}, E_a: 29.0 kJ mol^{-1}, ΔS: 0.655 kJ mol^{-1} K^{-1}, H_d: 209.0 kJ mol^{-1}; d) M2002: k_{25}: 68.9 µmol m^{-2} s^{-1}, E_a: 0.0 kJ mol^{-1}, ΔS: 0.746 kJ mol^{-1} K^{-1}, H_d: 240.5 kJ mol^{-1}; J1942: k_{25}: 69.5 µmol m^{-2} s^{-1}, E_a: 0.0 kJ mol^{-1}, ΔS: 0.625 kJ mol^{-1} K^{-1}, H_d: 201.0 kJ mol^{-1}; e) M2002: k_{25}: 37.6 µmol m^{-2} s^{-1}, E_a: 57.7 kJ mol^{-1}, ΔS: 0.579 kJ mol^{-1} K^{-1}, H_d: 185.4 kJ mol^{-1}; J1942: k_{25}: 37.0 µmol m^{-2} s^{-1}, E_a: 57.7 kJ mol^{-1}, ΔS: 0.557 kJ mol^{-1} K^{-1}, H_d: 178.1 kJ mol^{-1}; f) M2002: k_{25}: 66.7 µmol m^{-2} s^{-1}, E_a: 23.0 kJ mol^{-1}, ΔS: 0.761 kJ mol^{-1} K^{-1}, H_d: 246.6 kJ mol^{-1}; J1942: k_{25}: 65.5 µmol m^{-2} s^{-1}, E_a: 23.0 kJ mol^{-1}, ΔS: 0.668 kJ mol^{-1} K^{-1}, H_d: 216.1 kJ mol^{-1}.

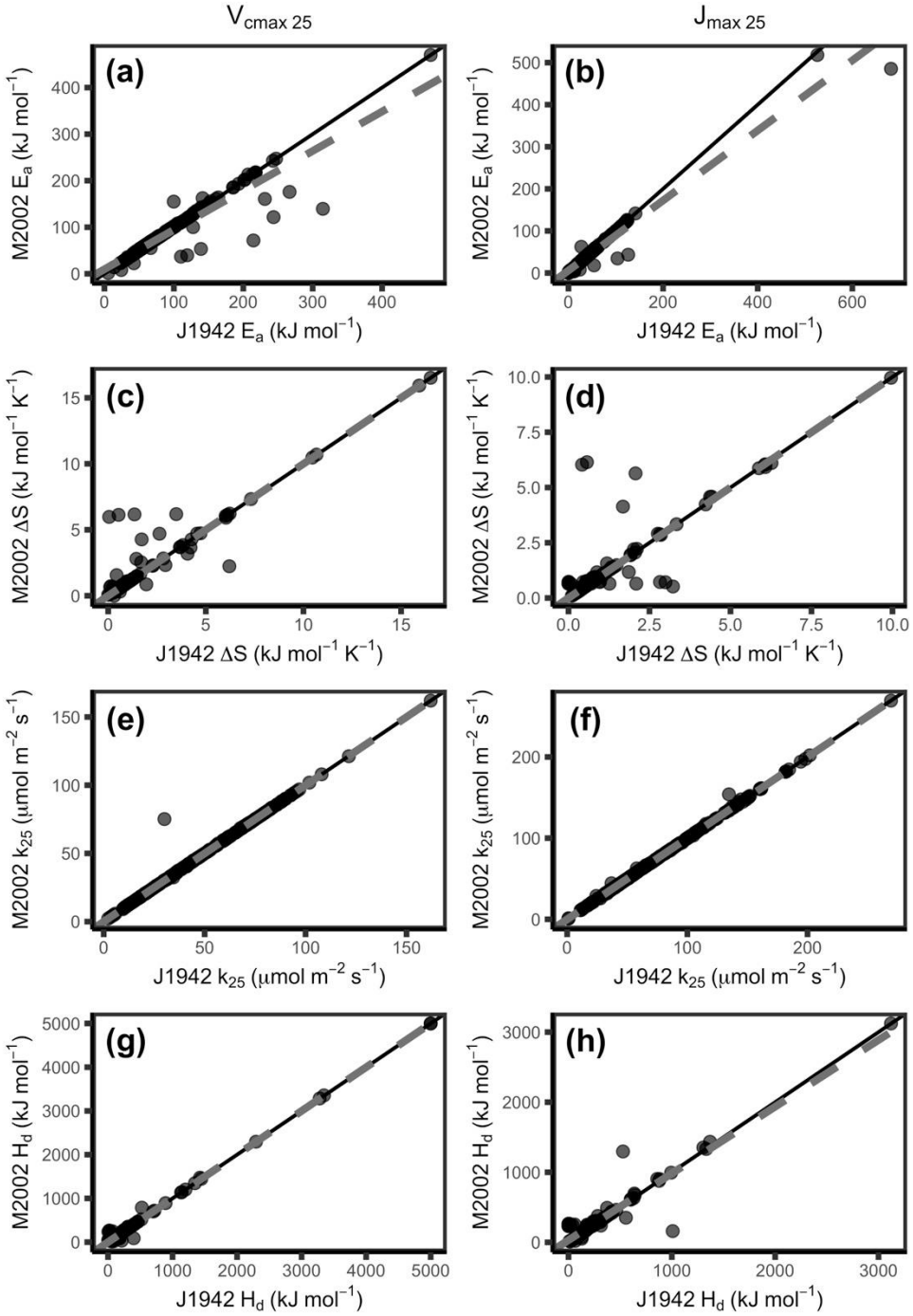

Figure 2. The modified Arrhenius equation missing the term (M2002) compared to J1942 fits different values for E_a (a,b), but mostly similar values for ΔS (c,d), k_{25} (e,f) and H_d (f, g) for both V_{cmax} (a, c, e, g) and J_{max} (c, d, f, h). E_a: activation energy, ΔS: entropy parameter, k_{25}: rate of the process at 25 °C, H_d: deactivation energy, V_{cmax}: maximum capacity of rubisco carboxylation, J_{max}: maximum rate of electron transport. Black line indicates 1:1 line and grey dashed line indicates respective modelled slopes and intercepts.

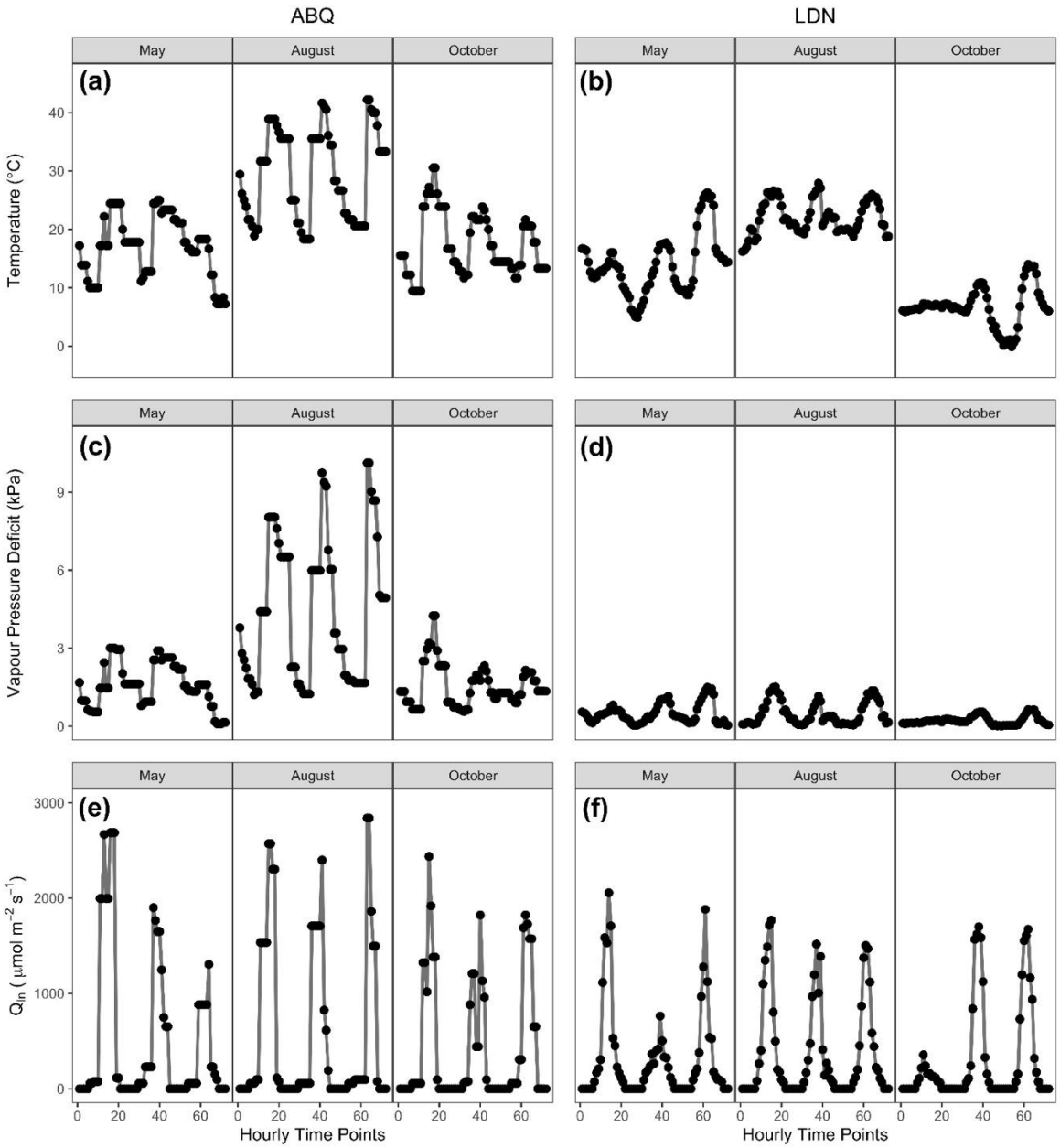

Figure 3. Hourly environmental data used to drive the model in Table 3 covering 3 days (17th, 18th, and 19th) of 3 months. (a,c,e) Albuquerque, NM, USA (ABQ); (b,d,e) London, ON, Canada (LDN). Environmental parameters include: a,b) temperature; c,d) vapour pressure deficit; and e,f) irradiance (Q_{in}).

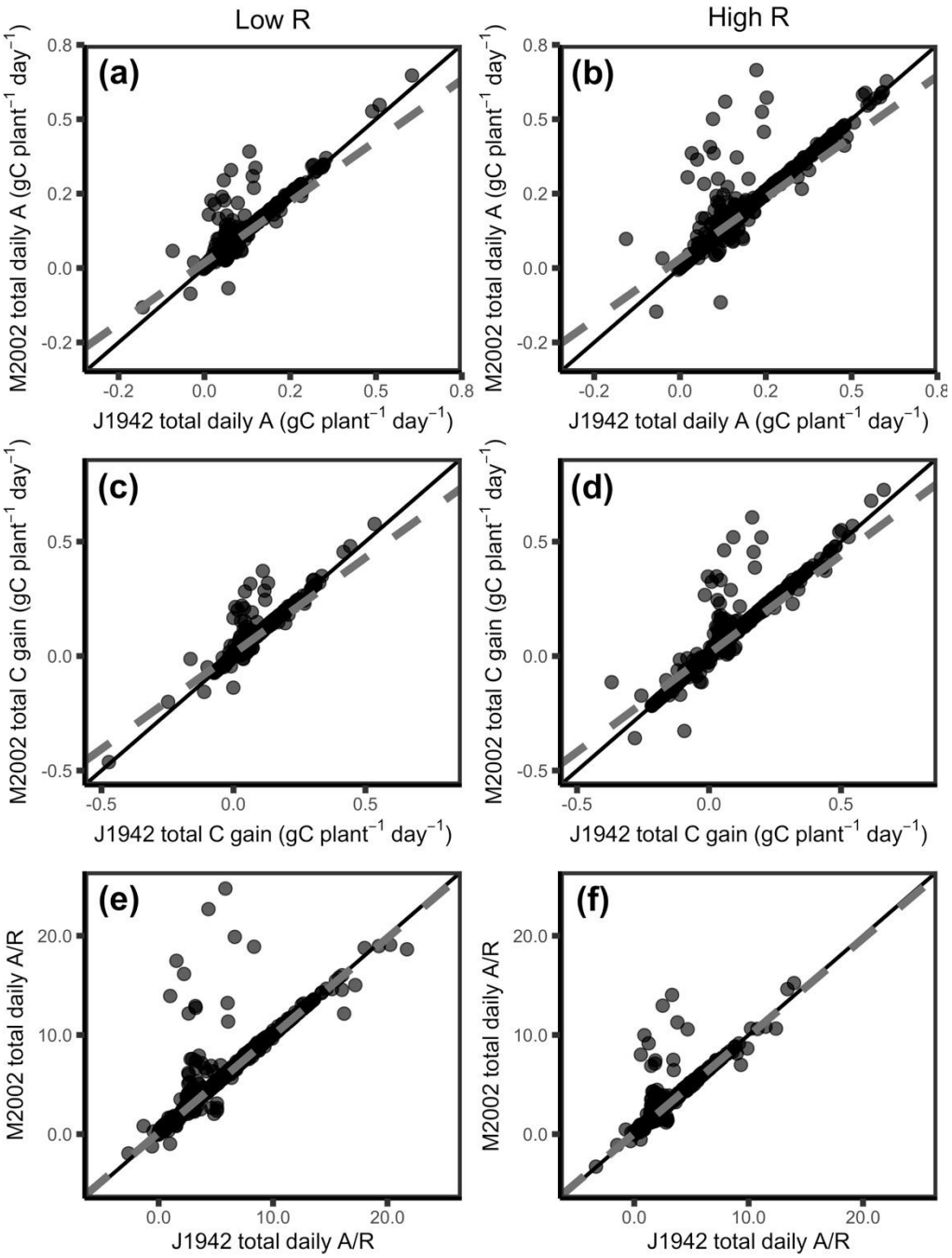

Figure 4. The modified Arrhenius equation without the missing term (M2002) gives differences in modelled daily carbon fluxes compared to J1942 for low R (a,c,e) and high R (b,d,f) under scenarios where H_d is allowed to vary. Modelled carbon fluxes include: a,b) Total daily photosynthesis; c,d) total daily C gain; and e,f) total daily A/R. A: photosynthesis, R respiration, Low R: low respiration, High R: high respiration. Black line indicates 1:1 line and grey dashed line indicates respective modelled slopes and intercepts.

References

Amthor JS. 2000. Direct effect of elevated CO_2 on nocturnal in situ leaf respiration in nine temperate deciduous tree species is small. *Tree Physiology* **20**: 139–144.

Arora VK, Katavouta A, Williams RG, Jones CD, Brovkin V, Friedlingstein P, Schwinger J, et al. 2020. Carbon-concentration and carbon-climate feedbacks in CMIP6 models, and their comparison to CMIP5 models. *Biogeosciences* doi: 10.5194/bg-2019-473.

Arrhenius S. 1915. *Quantitative laws in biological chemistry*. Bell: London.

Atkin OK, Tjoelker MG. 2003. Thermal acclimation and the dynamic response of plant respiration to temperature. *Trends in Plant Science* **8**:343-351.

Ayub G, Smith RA, Tissue DT, Atkin OK. 2011. Impacts of drought on leaf respiration in darkness and light in *Eucalyptus saligna* exposed to industrial-age atmospheric CO_2 and growth temperature. *New Phytologist* **190**: 1003-1018.

Bernacchi CJ, Singsaas EL, Pimentel C, Portis Jr AR, Long SP. 2001. Improved temperature response functions for models of rubisco-limited photosynthesis. *Plant Cell and Environment* **24**:253-259.

Blackman, VH. 1919. The compound interest and plant growth. *Annals of Botany* **33:** 353-360.

Bonan GB. 1996. A Land Surface Model (LSM Version 1.0) for Ecological, Hydrological, and Atmospheric Studies: Technical Description and User's Guide (No. NCAR/TN-417+STR). *University Corporation for Atmospheric Research.* doi:10.5065/D6DF6P5X

Calvet J-C, Noilhan J, Roujean J-L, Bessemoulin P, Cabelguenne M, Olioso A, Wigneron J-P. 1998. An interactive vegetation SVAT model tested against data from six contrasting sites. *Agricultural and Forest Meteorology* **92**:73-95

Cao J, Wang B, Yang Y-M, Ma L, Li J, Sun B, Bao Y, He J, Zhou X, Wu L. 2018. The NUIST Earth System Model (NESM) version 3: description and preliminary evaluation. *Geoscientific Model Development* **11**:2975-2993.

Causton, DR. 1991. Plant-growth analysis: the variability of relative growth rate within a sample. *Annals of Botany* **67**(2): 137-144.

Ciais P, Sabine C, Bala G, Bopp L, Brovkin V, Canadell J, Chhabra A, DeFries R, Galloway J, Heimann M. 2013. Carbon and Other Biogeochemical Cycles. In: Heinze C, Tans P, Vesala T, eds. *Climate Change 2013: The Physical Science Basis.* Cambridge, UK, and New York, NY, USA: Cambridge University Press.

Clark DB, Mercado LM, Sitch S, Jones CD, Gedney N, Best MJ, Pryor M, et al. 2011. The Joint UK Land Environment Simulator (JULES), model description – part 2: carbon fluxes and vegetation dynamics. *Geoscientific Model Development* **4**:701-722.

Drake JE, Tjoelker MG, Aspinwall MJ, Reich PB, Pfautsch S, Barton CVM. 2019. The partitioning of gross primary production for young *Eucalyptus tereticornis* trees under experimental warming and altered water availability. *New Phytologist* **222:** 1298-1312

Duursma RA. 2015. Plantecophys – an R package for analysing and modelling leaf gas exchange data. *PLoS ONE* **10**:e0143346.

Duursma RA, Medlyn BE. 2012. MAESPA: a model to study interaction between water limitation, environmental drivers and vegetation function at tree and stand levels, with an example application to [CO_2] x drought interactions*. Geoscientific Model Development* **5**:919-940.

Elzhov TV, Mullen KM, Spiess A-N, Bolker B. 2016. minpack.lm: R Interface to the Levenberg-Marquardt nonlinear least-squares algorithm found in MINPACK, plus support for bounds. R package version 1.2-1. https://CRAN.R-project.org/package=minpack.lm

Farquhar GD, von Caemmerer S, Berry JA. 1980. A biochemical model of photosynthetic CO_2 assimilation in leaves of C_3 species. *Planta* **149**: 78-90.

Friend AD, Kiang NY. 2005. Land surface model development for the GISS GCM: effects of improved canopy physiology on simulated climate. *Journal of Climate* **18**:2883-2902.

Hall AE. 1979. A model of leaf photosynthesis and respiration for predicting carbon dioxide assimilation in different environments. *Oecologia* **43**: 299-316.

Harley PC, Baldocchi DD. 1995. Scaling carbon dioxide and water vapour exchange from leaf to canopy in a deciduous forest. I. Leaf model parameterization. *Plant, Cell and Environment* **18**:1146-1156.

Harley PC, Thomas RB, Reynolds JF, Strain BR. 1992. Modelling photosynthesis of cotton grown in elevated CO_2. *Plant, Cell and Environment* **15**:271-282.

Harley PC, Tenhunen JD, Lange OL. 1986. Use of an analytical model to study limitations on net photosynthesis in *Arbutus unedo* under field conditions. *Oecologia* **70**:393-401.

Haverd V, Smith B, Nieradzik L, Briggs PR, Woodgate W, Trudinger CM, Canadell JG, Cuntz M. 2018. A new version of the CABLE land surface model (Subversion revision r4601) incorporating land use and land cover change, woody vegetation demography, and a novel optimization-based

approach to plant coordination of photosynthesis. *Geoscientific Model Development* **11**:2995-3026.

Heskel MA, O'Sullivan OS, Reich PB, Tjoelker MG, Weerasinghe LK, Penillard A, Egerton JJG, et al. 2016. Convergence in the temperature response of leaf respiration across biomes and plant functional types. *Proceedings of the National Academy of Sciences USA* **113**: 3832-3837.

Hobbs JK, Jiao W, Ester AD, Parker EJ, Schipper LA, Arcus VL. 2013. Change in heat capacity for enzyme catalysis determines temperature dependence of enzyme catalyzed rates. *ACS Chemical Biology* **8**:2388-2392.

Hosaka M. 2011. A new MRI land surface model HAL. *AGU Fall Meeting Abstracts* GC43B-0901.

Ito A. 2020. Changing ecophysiological processes and carbon budget in East Asian ecosystems under near-future changes in climate: implications for long-term monitoring from a process-based model. *Journal of Plant Research* **123**:577-588.

Jensen JLWV. 1906. Sur les fonctions convexes et les inégalités entre les valeurs moyennes. *Acta Mathematica* **30**: 175-193.

Ji J. 1995. A climate-vegetation interaction model: simulating physical and biological processes at the surface. *Journal of Biogeography* **22**:445-451.

Joetzjer E, Delire C, Douville H, Ciais P, Decharme B, Carrer D, Verbeeck H, De Weirdt M, Bonal D. 2015. Improving the $ISBA_{CC}$ land surface model simulation of water and carbon fluxes and stocks over the Amazon forest. *Geoscientific Model Development* 8:1709-1727.

Johnson FH, Eyring H, Williams RW. 1942. The nature of enzyme inhibitions in bacterial luminescence: sulfanilamide, urethane, temperature and pressure. *Journal of Cellular and Comparative Physiology* **20**:247-268.

Kattge J, Knorr W. 2007. Temperature acclimation in a biochemical model of photosynthesis: a reanalysis of data from 36 species. *Plant, Cell and Environment* **30**:1176-1190.

Kruse J, Hopmans P, Adams MA. 2008. Temperature responses are a window to the physiology of dark respiration: differences between CO_2 release and O_2 reduction shed light on energy conservation. *Plant, Cell and Environment* **31**: 901-914.

Kumarathunge DP, Medlyn BE, Drake JE, Tjoelker MG, Aspinwall MJ, Battaglia M, Cano FJ, Carter KR, Molly AC, Lucas AC, et al. 2019. Acclimation and adaptation components of the

523 temperature dependence of plant photosynthesis at the global scale. *New Phytologist* **222**:768-
524 784.
525 **Kumarathunge DP, Medlyn BE, Drake JE, Tjoelker MG, Aspinwall MJ, Battaglia M, Cano FJ, Carter**
526 **KR, Molly AC, Lucas AC, et al. 2018.** ACi-TGlob_V1.0: a global dataset of photosynthetic CO_2
527 response curves of terrestrial plants. doi: 10.6084/m9.figshare.7283567.v1.
528 **Lawrence D, Fisher R, Koven C, Oleson K, Swenson S, Vertenstein M, et al. 2018.** Technical
529 Description of version 5.0 of the Community Land Model (CLM). National Center for
530 Atmospheric Research. http://www.cesm.ucar.edu/models/cesm2/land/
531 **Lloyd J, Grace J, Miranda AC, Meir P, Wong SC, Miranda HS, Wright IR, Gash JHC, McIntyre J. 1995.** A
532 simple calibrated model of Amazon rainforest productivity based on leaf biochemical
533 properties. *Plant, Cell and Environment* **18**:1129-1145.
534 **Lombardozzi DL, Bonan GB, Smith NG, Dukes JS, Fisher RA. 2015.** Temperature acclimation of
535 photosynthesis and respiration: a key uncertainty in the carbon cycle-climate feedback.
536 *Geophysical Research Letters* **42**:8624-8631.
537 **Loveys BR, Atkinson LJ, Sherlock DJ, Roberts RL, Fitter AH, Atkin OK. 2003.** Thermal acclimation of
538 leaf and root respiration: An investigation comparing inherently fast- and slow-growing plant
539 species. *Global Change Biology* **9**(6): 895-910.
540 **Medlyn BE, Duursma RA, Eamus D, Ellsworth DS, Prentice IC, Barton CVM, Crous KY, et al. 2011.**
541 Reconciling the optimal and empirical approaches to modelling stomatal conductance. *Global*
542 *Change Biology* **17**:2134-2144.
543 **Medlyn BE, Dreyer E, Ellsworth D, Forstreuter M, Harley PC, Kirschbaum MUF, Le Roux X, et al.**
544 **2002.** Temperature responses of parameters of a biochemically based model of photosynthesis.
545 II. A review of experimental data. *Plant, Cell and Environment* **25**:1167-1179.
546 **Milly PCD, Malyshev SL, Shevliakova E, Dunne KA, Findell KL, Gleeson T, Liang Z, et al. 2014.** An
547 enhanced model of land water and energy for global hydrologic and Earth-system studies.
548 *Journal of Hydrometeorology* **15**:1739-1761.
549 **Norman JM, Campbell GS. 1998.** *An introduction to environmental biophysics*. New York NY: Springer.
550 **Pommerening A, Muszta, A. 2015.** Methods of modelling relative growth rate. *Forest Ecosystems* **2**:5.

Poorter H, Niklas KJ, Reich PB, Oleksyn J, Poot P, Mommer L. 2012. Biomass allocation to leaves, stem, and roots: meta-analyses of interspecific variation and environmental control. *New Phytologist* **193**: 30-50.

R Core Team. 2019. R: A language and environment for statistical computing. R Foundation for Statistical Computing, Vienna, Austria. URL https://www.R-project.org/.

Rogers A, Medlyn BE, Dukes JS, Bonan G, von Caemmerer S, Dietze MC, Kattge J, et al. 2017. A roadmap for improving the representation of photosynthesis in Earth system models. *New Phytologist* **213**:22-42.

Sato N, Sellers PJ, Randall DA, Schneider EK, Shukla J, Kinter JL, Hou Y-T, Albertazzi E. 1989. Implementing the Simple Biosphere Model (SiB) in a general circulation model: methodologies and results. *NASA Technical Report* NASA-CR-185509.

Sharpe PJH, DeMichele DW. 1977. Reaction kinetics of poikilotherm development. *Journal of Theoretical Biology* **64**: 649-670.

Shipley, B. 1989. The use of above-ground maximum relative growth-rate as an accurate predictor of whole-plant maximum relative growth-rate. *Functional Ecology* **3**(6): 771-775.

Sitch S, Smith B, Prentice IC, Arneth A, Bondeau A, Cramer W, Kaplan JO, et al. 2003. Evaluation of ecosystem dynamics, plant geography and terrestrial carbon cycling in the LPJ dynamic global vegetation model. *Global Change Biology* **9**:161-185.

Smith NG, Dukes JS. 2017. Short-term acclimation to warmer temperatures accelerates leaf carbon exchange processes across plant types. *Global Change Biology* **23**:4840-4853.

Stinziano JR, Murphy BK. 2020. arrhenius.comparison: comparing versions of the modified Arrhenius equation. R package version 1.0.2. https://github.com/jstinzi/arrhenius.comparison.

Stinziano JR, Way DA. 2017. Autumn photosynthetic decline and growth cessation in seedlings of white spruce are decoupled under warming and photoperiod manipulations. *Plant, Cell and Environment* **40:**1296-1316.

Stinziano JR, Way DA, Bauerle WL. 2018. Improving models of photosynthetic thermal acclimation: which parameters are most important and how many should be modified? *Global Change Biology* **24**:1580-1598.

Stinziano JR, Bauerle WL, Way DA. 2019. Modelled net carbon gain responses to climate change in boreal trees: impacts of photosynthetic parameter selection and acclimation. *Global Change Biology* **25**:1445-1465.

Swart NC, Cole JNS, Kharin VV, Lazare M, Scinocca JF, Gillett NP, Anstey J, et al. 2019. The Canadian Earth System Model version 5 (CanESM5.0.3). *Geoscientific Model Development* **12:**4823-4873.

Tjoelker M, Oleksyn J, Reich P. 1999. Acclimation of respiration to temperature and CO_2 in seedlings of boreal tree species in relation to plant size and relative growth rate. *Global Change Biology* **49**(6): 679-691.

Volodin EM, Lykosov VN. 1998. Parameterization of heat and moisture transfer in the soil-vegetation system for use in atmospheric general circulation models: 1. Formulation and simulations based on local observational data. *Izvestiya Atmospheric and Oceanic Physics* **34:**405-416.

Way DA, Yamori W. 2014. Thermal acclimation of photosynthesis: on the importance of adjusting our definitions and accounting for thermal acclimation of respiration. *Photosynthesis Research* **119**:89-100.

Weger HG, Guy RD. 1991. Cytochrome and alternative pathway respiration in white spruce (*Picea glauca*) roots. Effects of growth and measurement temperature. *Physiologia Plantarum* **83**:675-681.

Supplementary information

Appendix A – Alternate derivations of the modified Arrhenius equation

Below are the temperature relativizations of Farquhar et al. (1980), Harley et al. (1986), and Harley et al. (1992) showing that Farquhar et al. (1980) and Harley et al. (1992) can be transformed to be identical to Equation 3 in the manuscript, while Harley et al. (1986) can be transformed to be identical to Equation 10 in the manuscript.

Farquhar et al. (1980)

From Eq. 36 in Farquhar et al. (1980):

$$k = \frac{\mathrm{c} \times \exp\left[-E/(RT_k)\right]}{1+\exp\left[(ST_k - H)/(RT_k)\right]} \qquad \text{Equation A1}$$

Relativizing to 25 °C:

$$k/k_{25} = \left[\frac{\mathrm{c} \times \exp\left[-E/(RT_k)\right]}{1+\exp\left[(ST_k - H)/(298.15R)\right]}\right]\left[\frac{1+\exp\left[(ST_k - H)/(298.15R)\right]}{\mathrm{c} \times \exp\left[-E/(T_k R)\right]}\right] \qquad \text{Equation A2}$$

Simplifying:

$$k/k_{25} = \exp\left[E/(298.15R) - E/(RT_k)\right]\left[\frac{1+\exp\left[(S298.15 - H)/(298.15R)\right]}{1+\exp\left[(ST_k - H)/(RT_k)\right]}\right] \qquad \text{Equation A3}$$

$$k = k_{25} \exp\left[E\,\frac{(T_k - 298.15)}{(298.15RT_k)}\right]\left[\frac{1+\exp\left[(298.15S - H)/(298.15R)\right]}{1+\exp\left[(ST_k - H)/(RT_k)\right]}\right] \qquad \text{Equation A4}$$

where E is activation energy (E_a), S is deactivation entropy (ΔS), and H is deactivation energy (H_d).

Harley et al. (1986)

From Eq. 7 in Harley et al. (1986):

$$k = \frac{T_k \exp\left[c - \Delta H_a/(RT_k)\right]}{1+\exp\left[(\Delta ST_k - \Delta H_d)/(RT_k)\right]} \qquad \text{Equation A5}$$

Relativizing to 25 °C:

$$k/k_{25} = \left[\frac{T_k \exp\left[c - \Delta H_a/(RT_k)\right]}{1+\exp\left[(\Delta ST_k - \Delta H_d)/(RT_k)\right]}\right]\left[\frac{1+\exp\left[(\Delta S298.15 - \Delta H_d)/(R298.15)\right]}{298.15 \exp\left[c - \Delta H_a/(R298.15)\right]}\right] \qquad \text{Equation A6}$$

Simplifying:

$$k/k_{25} = \frac{T_k}{298.15} \exp\left[\Delta H_a/(R298.15) - \Delta H_a/(RT_k)\right] \left[\frac{1+\exp\left[(\Delta S298.15-\Delta H_d)/(R298.15)\right]}{1+\exp\left[(\Delta ST_k-\Delta H_d)/(RT_k)\right]}\right] \quad \text{Equation A7}$$

$$k = k_{25} \frac{T_k}{298.15} \exp\left[\Delta H_a \frac{(T_k-298.15)}{(298.15RT_k)}\right] \left[\frac{1+\exp\left[(298.15\Delta S-\Delta H_d)/(298.15R)\right]}{1+\exp\left[(\Delta ST_k-\Delta H_d)/(RT_k)\right]}\right] \quad \text{Equation A8}$$

where ΔH_a is activation energy (E_a), and ΔH_d is deactivation energy (H_d).

Harley et al. (1992)

From Eq. 9 in Harley et al. (1992):

$$k = \frac{\exp\left[c-\Delta H_a/(RT_k)\right]}{1+\exp\left[(\Delta ST_k-\Delta H_d)/(RT_k)\right]} \quad \text{Equation A9}$$

Relativizing to 25 °C:

$$k/k_{25} = \left[\frac{\exp\left[c-\Delta H_a/(RT_k)\right]}{1+\exp\left[(\Delta ST_k-\Delta H_d)/(RT_k)\right]}\right] \left[\frac{1+\exp\left[(\Delta S298.15-\Delta H_d)/(R298.15)\right]}{\exp\left[c-\Delta H_a/(R298.15)\right]}\right] \quad \text{Equation A10}$$

Simplifying:

$$k/k_{25} = \exp\left[\Delta H_a/(R298.15) - \Delta H_a/(RT_k)\right] \left[\frac{1+\exp\left[(\Delta S298.15-\Delta H_d)/(R298.15)\right]}{1+\exp\left[(\Delta ST_k-\Delta H_d)/(RT_k)\right]}\right] \quad \text{Equation A11}$$

$$k = k_{25} \exp\left[\Delta H_a \frac{(T_k-298.15)}{(298.15RT_k)}\right] \left[\frac{1+\exp\left[(298.15\Delta S-\Delta H_d)/(298.15R)\right]}{1+\exp\left[(\Delta ST_k-\Delta H_d)/(RT_k)\right]}\right] \quad \text{Equation A12}$$

where ΔH_a is activation energy (E_a), and ΔH_d is deactivation energy (H_d).